

OXYGEN ISOTOPE DISTRIBUTION IN ANORTHITE-SPINEL-RICH INCLUSIONS FROM THE NINGQIANG CARBONACEOUS CHONDRITE.

Yunbin Guan¹, Yanting Lin² and Laurie A. Leshin^{1,3},
¹Department of Geological Sciences, Arizona State University, Box 871404, Tempe, AZ 85287-1404 USA (yunbin.guan@asu.edu); ²Institute of Geology and Geophysics, Chinese Academy of Sciences, P.O. Box 9825, Beijing 100029, China (liny@mail.igcas.ac.cn); ³Center for Meteorite Studies, Arizona State University, Box 871404, Tempe, AZ 85287-1404 USA (laurie.leshin@asu.edu).

Introduction: Ningqiang is an anomalous carbonaceous chondrite, with petrologic and chemical affinities to CK and CV chondrites. Bulk and *in situ* oxygen isotope analyses have been reported for its chondrule, matrix, and type A calcium-aluminum-rich inclusions (CAIs) [1-4]. In this study, we investigate the oxygen isotope compositions of another type of CAIs -- anorthite-spinel-rich inclusion (ASI) [5], in Ningqiang.

Samples and Analytical Techniques: We analyzed three CAIs from two polished thin sections of Ningqiang (NQJ1-1 and NQJ2-1). Two of the CAIs (NQJ1-1#1 and NQJ2-1#1) are irregular-shaped large (a few mm in size) ASIs previously described in [5]. They consist of a spinel-rich core, a spinel-anorthite-Ca-pyroxene mantle, and a melilite-spinel crust. Sodalite coexists with nepheline in the mantles in the ASIs, and both replace anorthite. The other CAI (NQJ1-1#2) is a small (~60 μ m in diameter) melilite-spinel inclusion with a diopside rim.

In-situ oxygen isotope analyses of individual components in Ningqiang CAIs were carried out using the Cameca IMS 6f ion microprobe at ASU, and techniques described in [6]. Uncertainties on individual analyses, taking into account the variation on repeated analyses of the standard, are ~1-2‰ (2 σ). Matrix effects are minor under our analysis conditions and no correction for such effects has been made.

Results: The oxygen isotope compositions of individual minerals in the three Ningqiang CAIs are plotted in Fig. 1. All the data plot along the CCAM line with spinel showing "typical" ¹⁶O-enriched $\delta^{18}\text{O}$ and $\delta^{17}\text{O}$ values at -40 to -50‰. Spinels in the mantle and core of the ASIs exhibit no obvious difference in their oxygen isotope compositions. The less ¹⁶O-enriched δ -values (-37‰ and -40‰) of two spinels, one in the crust of NQJ1-1#1 and the other in the center of NQJ1-1#2, result from slight beam overlap onto ¹⁶O-poor melilite (see following results) during analysis. Two diopside grains, one in the crust of NQJ1-1#1 and the other in the rim of NQJ1-1#2, contain intermediate ¹⁶O-excesses, plotting along the CCAM line at δ -values of about -30‰.

Two anorthite spots from the NQJ1-1#1 mantle have δ -values of ~ -15‰ and -12‰. Similar oxygen isotope compositions were observed in two melilite

grains separately located in the crust of NQJ1-1#1 and the center of NQJ1-1#2.

Sodalite in the mantle of NQJ1-1#1, which contains ³⁶S excesses from *in situ* decay of the short-lived radionuclide ³⁶Cl [7], is slightly less ¹⁶O-enriched than melilite and anorthite.

Intriguing oxygen isotopic data were observed for perovskite in the two Ningqiang ASIs. Perovskite grains in the two ASIs are normally about 10 μ m or less in size. They can be found enclosed in spinel, melilite, and diopside (e.g. Fig. 2; Fig. 3). The oxygen isotope compositions of six perovskite grains show large variations and generally are not enriched in ¹⁶O. Two perovskite grains in the NQJ1-1#1 core (Fig. 2), obviously formed earlier than spinel and showing no sign of late reaction, have δ -values of about -27‰. SEM examination of ion microprobe craters indicated slight overlap onto the surrounding spinel for these two spots. Two perovskites in the NQJ2-1#1 mantle (Fig. 3), probably endured a later alteration event during which anorthite and Ca-pyroxene replaced melilite to form the ASI mantle [5], give values of $\delta^{18}\text{O}$ =-5‰ and $\delta^{17}\text{O}$ =-10‰. Due to beam overlap, the δ -values ($\delta^{18}\text{O}$ =-16‰ and $\delta^{17}\text{O}$ =-17‰) of another perovskite grain of similar occurrence suffer from significant contribution from surrounding diopside, anorthite, and spinel grains. One grain from the crust of NQJ1-1#1, is the most ¹⁶O-depleted grain measured in this study, with $\delta^{18}\text{O}$ =5‰ and $\delta^{17}\text{O}$ =-2‰. Similarly ¹⁶O-depleted oxygen isotope compositions were previously reported for perovskite in type A CAIs from Leoville [8] and Ningqiang [4], and in a type B CAI from Allende [9].

Discussion: The oxygen isotope heterogeneity among spinel, diopside, melilite, anorthite, and sodalite in Ningqiang CAIs is generally similar to observations made in Allende CAIs [e.g. 10, 11], presumably produced by post-crystallization isotopic exchange between ¹⁶O-rich solids and ¹⁶O-poor nebular gas (or some other ¹⁶O-poor components). Ningqiang melilite, anorthite, and sodalite are somewhat less depleted in ¹⁶O than their counterparts in Allende CAIs [10, 11]. Anorthite in Ningqiang ASIs was formed by reaction of melilite with gaseous components [5], probably in a ¹⁶O-poor reservoir in the nebula. The intermediate ¹⁶O-excess of anorthite is consistent with its secondary ori-

gin. In addition, the reaction probably took place at least 1.5 My after formation of the original CAIs as indicated by the absence of ^{26}Mg -excess in anorthite. Sodalite in the Ningqiang CAIs was produced by alteration of anorthite, which happened not much later than the formation of anorthite, otherwise the short-lived ^{36}Cl should have decayed [7]. Sodalite shows only slightly less ^{16}O -excess than anorthite, suggesting a similar oxygen reservoir for both minerals.

Perovskite is believed to be one of the high temperature primary phases formed early in CAI condensation or crystallization sequences [e.g., 12, 13], and should consequently contain ^{16}O -enrichments like most hibonite and spinel. All the *in situ* measurements available [4, 8, 9, and this study], however, indicate that CAI perovskite is relatively ^{16}O -depleted. What could be the possible mechanisms that produced ^{16}O -poor perovskite? If originally ^{16}O -enriched, later partial melting might affect the perovskites in the type A CAI from Leoville [8] and the type B CAI from Allende [9], but little melting has been observed in the two ASIs [5] and the fluffy type A CAI [14] from Ningqiang. For later diffusion process to be the cause of ^{16}O -depletion in CAI perovskite, it requires very fast oxygen diffusion rate in perovskite. There is no experimental data available; however, if the oxygen diffusion rate in perovskite is similar to that in spinel, which is extremely slow, diffusion could not be the cause for ^{16}O -depletion in perovskite. In addition, the occurrence of ^{16}O -poor perovskite enclosed in ^{16}O -rich spinel is difficult to explain by diffusion processes. Another possibility is that perovskite are relict grains that formed with or without ^{16}O excesses before their incorporation into the CAIs, which implies that they originated from a separate CAI formation episode as for spinel and pyroxene, and probably from a different oxygen isotopic reservoir as well. Obviously, further systematic investigation is needed to understand the implications of the observed ^{16}O -depletion in CAI perovskite.

References: [1] Mayeda T. K. et al. (1988) *Meteoritics*, 23, 288. [2] Clayton R. N. and Mayeda T. K. (1999) *GCA*, 63, 2089-2104. [3] Choi B.-G. (2003) *GCA*, 67, 4655-4600. [4] Hiyagon et al. (2004) *MAPS*, 39, A46. [5] Lin Y. and Kimura M. (1998) *MAPS*, 33, 501-511. [6] Jones R. H. et al. (2004) *GCA*, 68, 3423-3438. [7] Lin Y. et al. (2005) *PNAS* (in press). [8] Caillat C. et al. (1997) *LPS XXVIII*, 199-200. [9] Kim G. L. et al. (2002) *J. Mineral. Petrol. Sci.*, 97, 161-167. [10] McKeegan K. D. and Leshin L. A. (2001) *Rev. Mineral. Geochem.*, 43, 279-318. [11] Yurimoto H. et al. (1994) *EPSL*, 128, 47-53. [12] Stolper E. (1982) *GCA*, 46, 2159-2180. [13] Beckett J. R. and Stolper E. (1994) *Meteoritics*,

29, 41-65. [14] Lin Y. and Kimura M. (2003) *GCA*, 67, 2251-2267.

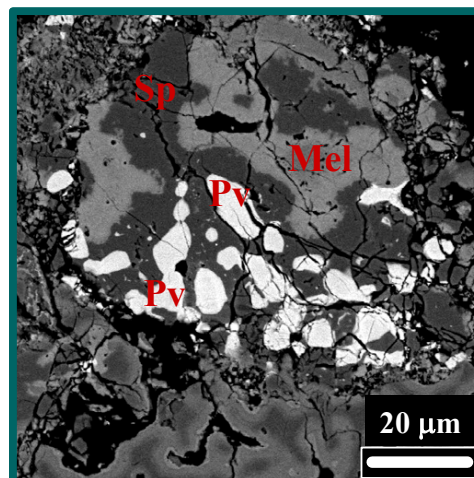
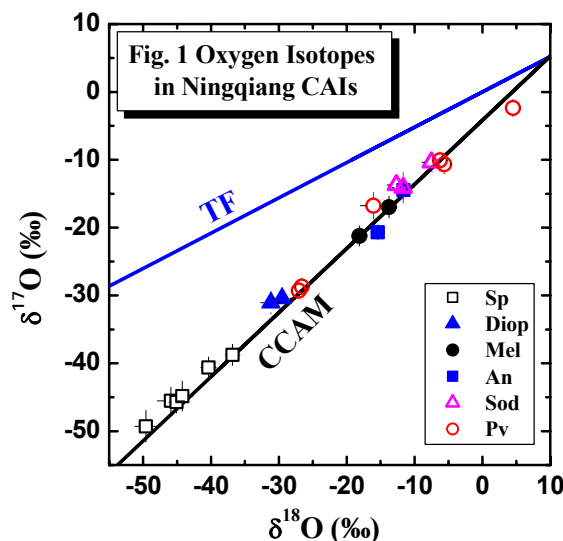


Fig. 2 Perovskite in the core of NQJ1-1#1

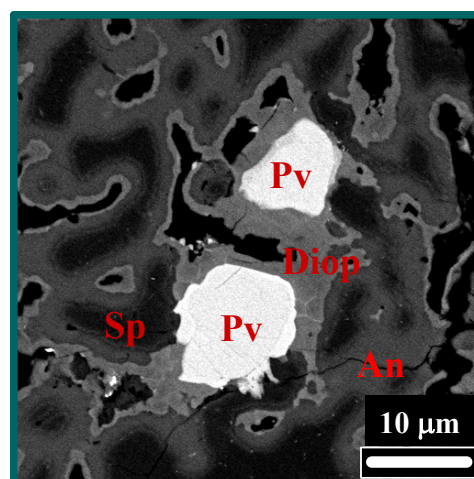


Fig. 3 Perovskite in the mantle of NQJ2-1#1